



AP-4 mediates export of ATG9A from the *trans*-Golgi network to promote autophagosome formation

Rafael Mattera^{a,1}, Sang Yoon Park^{a,1}, Raffaella De Pace^a, Carlos M. Guardia^a, and Juan S. Bonifacino^{a,2}

^aCell Biology and Neurobiology Branch, Eunice Kennedy Shriver National Institute of Child Health and Human Development, National Institutes of Health, Bethesda, MD 20892

Edited by Pietro De Camilli, Howard Hughes Medical Institute and Yale University, New Haven, CT, and approved November 6, 2017 (received for review October 2, 2017)

AP-4 is a member of the heterotetrameric adaptor protein (AP) complex family involved in protein sorting in the endomembrane system of eukaryotic cells. Interest in AP-4 has recently risen with the discovery that mutations in any of its four subunits cause a form of hereditary spastic paraplegia (HSP) with intellectual disability. The critical sorting events mediated by AP-4 and the pathogenesis of AP-4 deficiency, however, remain poorly understood. Here we report the identification of ATG9A, the only multispinning membrane component of the core autophagy machinery, as a specific AP-4 cargo. AP-4 promotes signal-mediated export of ATG9A from the *trans*-Golgi network to the peripheral cytoplasm, contributing to lipidation of the autophagy protein LC3B and maturation of preautophagosomal structures. These findings implicate AP-4 as a regulator of autophagy and altered autophagy as a possible defect in AP-4-deficient HSP.

adaptor protein complexes | AP-4 | protein sorting | ATG9A | autophagy

Protein coats associated with the cytosolic face of organellar membranes play critical roles in the selection of cargo and formation of transport carriers at various stages of the endomembrane system of eukaryotic cells (1). A subset of coat proteins belongs to the family of heterotetrameric adaptor protein (AP) complexes, including AP-1, AP-2, AP-3, AP-4, AP-5, the COPI-F subcomplex, and components of TSET (2, 3). All of these complexes are evolutionarily ancient and phylogenetically conserved, although some were lost in specific lineages. One of the more recently described and least well-understood AP complexes is AP-4. Like other members of the family, AP-4 consists of four subunits encoded by different genes: ϵ (*AP4E1*), $\beta 4$ (*AP4B1*), $\mu 4$ (*AP4M1*), and $\sigma 4$ (*AP4S1*) (4, 5) (Fig. 1A). The whole complex is structured as a core domain, with two extended hinge and ear domains (Fig. 1A). Unlike AP-1, AP-2, and AP-3, which interact with clathrin via their hinge and ear domains (6–8), AP-4 is part of a nonclathrin coat (4, 5). AP-4 is specifically associated with the *trans*-Golgi network (TGN) (4, 5), at least in part due to interaction with the GTP-bound form of the small GTPase Arf1 (9). AP-4 is required for the recruitment to the TGN of tepsin (also known as ENTHD2 or AP4AT) (10), an AP-4 accessory protein comprising an ENTH domain, a VHS domain, and a disordered C-terminal domain with two short peptide motifs that interact with the ear domains of AP-4 ϵ and $\beta 4$ (11, 12). AP-4 is thought to sort a subset of transmembrane cargos into transport carriers bound for post-Golgi compartments of the endomembrane system, such as endosomes and the plasma membrane. Among the cargos that have been shown to undergo AP-4-mediated sorting are the amyloid precursor protein (APP) (13–16), AMPA-type glutamate receptors (AMPA) (17), and the $\delta 2$ glutamate receptor protein (17, 18). Sorting involves recognition of sorting signals in the tails of the cargo proteins by the $\mu 4$ subunit of AP-4. In APP, the signal is the sequence YKFFE, which fits the canonical motif YXX \emptyset (where \emptyset is a hydrophobic amino acid) for binding to μ -subunits of AP complexes, but with an additional glutamate residue at the fifth position (13, 15) (Fig. 1A). Binding of AMPAR to $\mu 4$ is indirectly

mediated by a noncanonical YRYRF sequence in the receptor-associated, transmembrane AMPA receptor regulatory proteins (TARPs) (17). Finally, in the $\delta 2$ glutamate receptor protein, binding to $\mu 4$ depends on several phenylalanine residues in a noncanonical context (18).

Interest in AP-4 has recently risen because of the discovery of mutations in genes encoding each of the subunits of AP-4 in a subset of autosomal recessive hereditary spastic paraplegias (HSPs), namely, SPG47 (*AP4B1*/ $\beta 4$), SPG50 (*AP4M1*/ $\mu 4$), SPG51 (*AP4E1*/ ϵ), and SPG52 (*AP4S1*/ $\sigma 4$) (19–21). HSPs are a heterogeneous group of disorders that share the characteristic of lower limb spasticity, but vary by the absence or presence of additional features (22). In the case of AP-4 deficiency, these features include severe intellectual disability, microcephaly, seizures, and growth retardation (19–21). Another anatomical finding in AP-4-deficient patients is the presence of a thin corpus callosum, a characteristic feature of this particular HSP subset (19–21). Ablation of the gene encoding AP-4 $\beta 4$ in mouse resulted in subtle motor abnormalities along with axonopathy in the brain, particularly in Purkinje neurons of the cerebellum (17). Moreover, both Purkinje and hippocampal neurons exhibited missorting of the normally somatodendritic AMPAR to the axon, where the receptors accumulated in axonal swellings containing the autophagy marker LC3B (17). These findings led to the conclusion that AP-4 is involved in sorting of AMPAR from the TGN to the somatodendritic domain. The missorted AMPAR in AP-4 $\beta 4$ knockout (KO) neurons were proposed to be sequestered and

Significance

A family of adaptor protein (AP) complexes functions to sort transmembrane cargos at different stages of the endomembrane system of eukaryotic cells. AP-4 is one of the most recently described and least well-understood members of this family. Interest in this complex has risen because mutations in any of its four subunits cause a form of hereditary spastic paraplegia (HSP) with intellectual disability. In this study, we demonstrate that AP-4 sorts ATG9A, the only transmembrane component of the core autophagy machinery, from the *trans*-Golgi network to peripheral compartments. This sorting is required to promote the early steps of autophagosome formation. Our observations implicate AP-4 as an autophagy regulator and altered autophagy as an underlying defect in AP-4-deficient HSP.

Author contributions: R.M., S.Y.P., and J.S.B. designed research; R.M., S.Y.P., R.D.P., and C.M.G. performed research; R.M., S.Y.P., and R.D.P. contributed new reagents/analytic tools; R.M., S.Y.P., R.D.P., C.M.G., and J.S.B. analyzed data; and R.M., S.Y.P., R.D.P., and J.S.B. wrote the paper.

The authors declare no conflict of interest.

This article is a PNAS Direct Submission.

Published under the PNAS license.

¹R.M. and S.Y.P. contributed equally to this work.

²To whom correspondence should be addressed. Email: juan.bonifacino@nih.gov.

This article contains supporting information online at www.pnas.org/lookup/suppl/doi:10.1073/pnas.1717327114/-DCSupplemental.

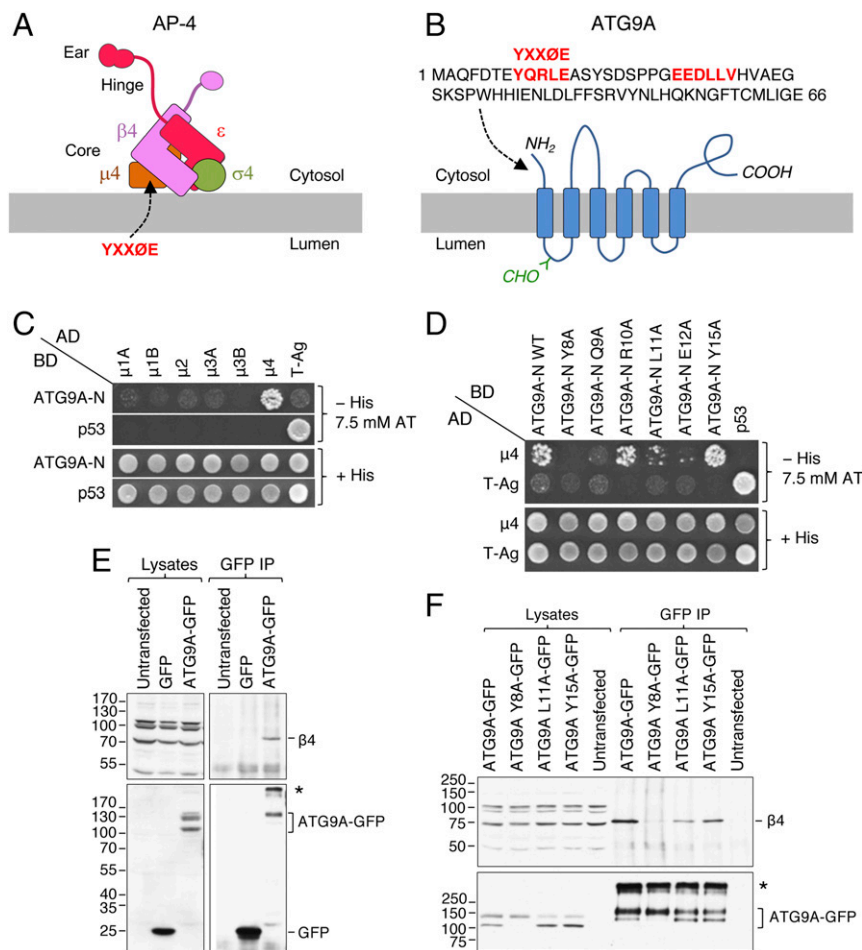


Fig. 1. Specific interaction of ATG9A with AP-4. (A) Schematic representation of the AP-4 complex depicting its subunits, structural domains, and recognition of YXXØE signals by the $\mu 4$ subunit. (B) Schematic representation of ATG9A showing the cytosolic, transmembrane, and luminal segments, an N-linked glycosylation site (CHO), and the sequence of the N-terminal (NH₂) cytosolic tail (amino acids 1–66 in human ATG9A). A consensus YXXØE motif (YQRLE) and a variant dileucine motif (EEDLLV) are highlighted in red. (C) Y2H analysis of the interaction of (i) the ATG9A N-terminal tail (ATG9A-N) fused to the Gal4 DNA binding domain (BD), with (ii) μ -subunits of different AP complexes fused to the Gal4 transcriptional activation domain (AD). p53 and T antigen (T-Ag) were used as controls. Growth in the absence of histidine (–His) and presence of 3-amino-1,2,4-triazole (AT) is indicative of interactions. Growth in the presence of histidine (+His) is a control for viability and loading of yeast double transformants. Images shown are composites of plates from the same experiment. (D) Y2H analysis of the interaction of: (i) ATG9A N-terminal tail constructs with different alanine substitutions fused to Gal4 BD, with (ii) $\mu 4$ fused to Gal4 AD, as described for C. (E) H4 cells stably expressing TSF-tagged AP-4 ϵ used in the original affinity purification and mass spectrometry analyses (11) were transiently transfected with plasmids encoding GFP or ATG9A-GFP. Detergent extracts were subjected to immunoprecipitation with antibody to GFP, and both lysates (2.8% of input) and immunoprecipitates were analyzed by immunoblotting with antibodies to AP-4 $\beta 4$ (Top) and GFP (Bottom). The positions of molecular mass markers are indicated on the Left, and those of the target proteins on the Right. The asterisk indicates aggregated ATG9A, a common occurrence for multispanning membrane proteins. (F) Coimmunoprecipitation of AP-4 $\beta 4$ with ATG9A bearing alanine substitutions in the N-terminal cytosolic tail was analyzed as described in E (lysate samples correspond to 1.4% of input). The complete list of proteins identified by mass spectrometry from the AP-4 ϵ tandem affinity purification is shown in Dataset S1.

degraded within axonal autophagosomes (17). The mislocalization and subsequent degradation of AMPAR might underlie at least some of the symptoms in AP-4-deficient HSP; however, it remains to be determined whether altered autophagy could also play a role in the pathogenesis of this disorder.

In the present study, we provide a direct link between AP-4 and autophagy. Using a combination of biochemical and functional analyses, we demonstrate that the autophagy protein ATG9A (Fig. 1B) is a physiological cargo of AP-4. ATG9A is the only multi-spanning membrane component of the core autophagy machinery (23). It normally cycles between the TGN and peripheral structures, including endosomes and preautophagosomal structures (PAS) to deliver membranes to the forming autophagosome (24–27). We find that the ATG9A–AP-4 interaction is mediated by binding of a conserved YXXØE motif (YQRLE) in the N-terminal cytosolic tail of ATG9A to the $\mu 4$ subunit of AP-4.

KO or knockdown (KD) of AP-4 subunits in various cell types causes retention of ATG9A in the TGN and its depletion from peripheral locations. AP-4-deficient cells exhibit decreased LC3B-II to LC3B-I ratios and accumulation of LC3B in atypical PAS under starvation conditions. These findings demonstrate that AP-4 is required for delivery of ATG9 to sites of autophagosome formation, thereby contributing to the maintenance of autophagic function. We propose that altered autophagy might underlie at least some of the symptoms of AP-4-deficient HSP.

Results

Identification of ATG9A as an AP-4-Interacting Protein. In a previous study (11), we performed tandem affinity purification (TAP) using as bait the ϵ subunit of AP-4 appended with an N-terminal Two-Strep/one FLAG (TSF) tag and expressed by stable transfection of H4 human neuroglioma cells. Copurifying proteins

were identified by mass spectrometry and scored using the contaminant repository for affinity purification (CRAPome) tool (28) (www.crapome.org/) to eliminate frequent contaminants (Dataset S1). Setting a stringent filter of zero appearances in 411 control purifications, the top hits were the four subunits of AP-4 and the AP-4 accessory protein tepsin (11) (highlighted in green in Dataset S1). Another hit that satisfied this criterion, but was not characterized in the previous study, was the autophagy protein ATG9A (Fig. 1B). ATG9A is a ubiquitously expressed, multispinning membrane protein that cycles between the TGN and peripheral cytoplasmic sites (24–27). It comprises six transmembrane helices with five connecting loops and N- and C-terminal tails facing the cytosol (25) (Fig. 1B). The N-terminal tail harbors a canonical YXXØ motif (where Ø is a bulky hydrophobic amino acid) (29) and a noncanonical LL motif (Fig. 1B) that mediate interactions with AP-1 and AP-2 (27, 30). These motifs as well as AP-1 and AP-2 were implicated in ATG9A traffic and/or autophagy (27, 30–33). Notably, the YXXØ motif in ATG9A is followed by a glutamate residue (YQRLE, amino acids 8–12), a distinct characteristic of a subset of YXXØ sequences that preferentially bind to the μ 4 subunit of AP-4 (13). Indeed, yeast two-hybrid (Y2H) analyses showed that the N-terminal tail of ATG9A (ATG9A-N) preferentially bound to μ 4 among the μ subunits of

several AP complexes (Fig. 1C). This binding was dependent on Y8, Q9, L11, and E12, but not R10, within the YQRLE sequence (Fig. 1D). It was also independent of another tyrosine, Y15, within a noncanonical sequence (Fig. 1D). Furthermore, ATG9A interacted with the whole AP-4 complex, as shown by coimmunoprecipitation of transiently expressed ATG9A-GFP, but not GFP, with the endogenous β 4 subunit of AP-4 in H4 cells stably transfected with AP-4 ϵ (Fig. 1E). In agreement with the Y2H results, this coimmunoprecipitation was also dependent on Y8, partially on L11, and less dependent on Y15 (Fig. 1F). From these experiments, we concluded that ATG9A is a bona fide AP-4 interactor that binds through a YXXØE motif in its N-terminal tail to the μ 4 subunit of AP-4.

ATG9A and AP-4 Colocalize at the TGN. Immunofluorescence microscopy for endogenous ATG9A and AP-4 ϵ in wild-type (WT) HeLa cells revealed localization of both molecules to a juxtannuclear structure, as well as to puncta scattered throughout the cytoplasm (Fig. 2A). KO of the gene encoding ATG9A abolished ATG9A staining at both the juxtannuclear and peripheral structures (Fig. 2A), indicating that they all reflect specific ATG9A localization. In contrast, KO of the AP-4 ϵ gene abrogated the juxtannuclear but not the peripheral AP-4 ϵ staining (Fig. 2A),

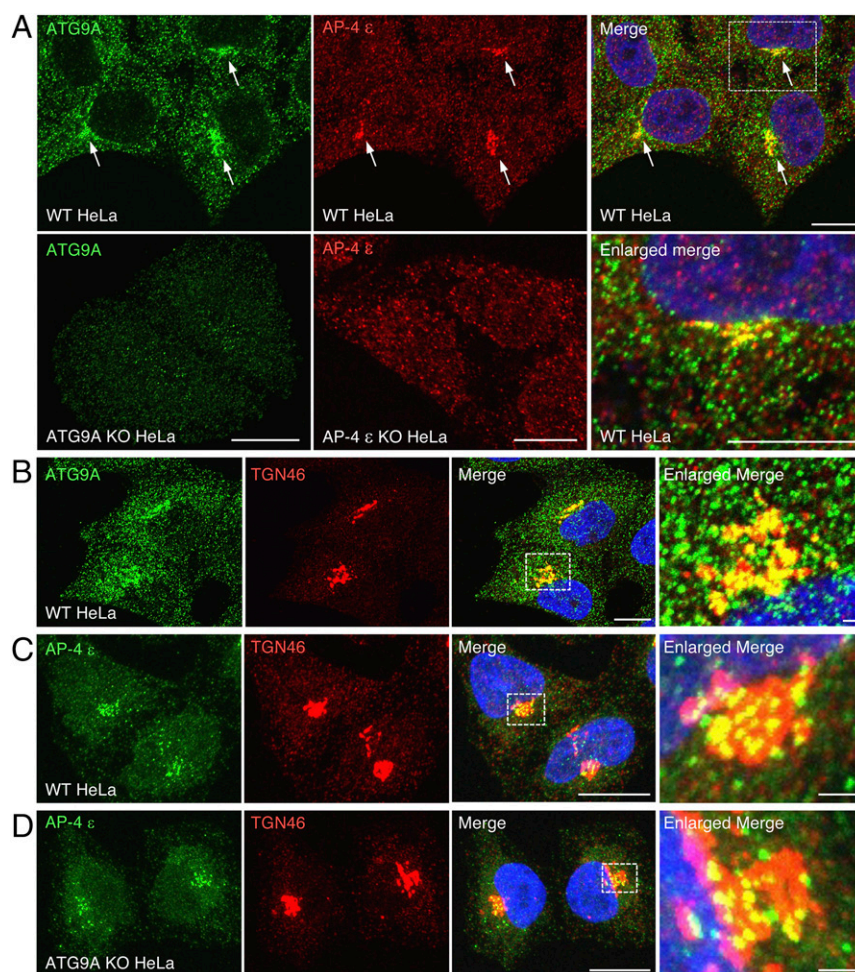


Fig. 2. Colocalization of ATG9A and AP-4 at the TGN. (A) Immunofluorescence microscopy of endogenous ATG9A and AP-4 ϵ in WT, ATG9A KO, and AP-4 ϵ KO cells. Arrows point to TGN structures containing both ATG9A and AP-4 ϵ . The *Bottom Right* image is an enlargement of the box in the *Top Right* image. (Scale bars, 10 μ m.) (B–D) Immunofluorescence microscopy colocalization of endogenous ATG9A and TGN46 in WT HeLa cells (B), AP-4 ϵ and TGN46 in WT HeLa cells (C), and AP-4 ϵ and TGN46 in ATG9A KO HeLa cells (D). Images in the *Right* column are enlargements of the boxed areas. (Scale bars, 10 μ m; enlarged images in B–D, 1 μ m.)

demonstrating that only the juxtannuclear staining is specific. Merging of the ATG9A and AP-4 images in WT HeLa cells showed partial colocalization of these proteins on the juxtannuclear structure (Fig. 2*A*). The juxtannuclear population of both ATG9A and AP-4 largely colocalized with the TGN marker TGN46 (Fig. 2*B* and *C*). These results are consistent with previous demonstrations of the localization of both AP-4 and ATG9A to the TGN (4, 5, 25) and with the additional localization of ATG9A to peripheral structures corresponding to endosomes and PAS (24–27). Taken together, these results are consistent with the interaction of ATG9A with AP-4 occurring at the TGN.

Depletion of AP-4 Causes Accumulation of ATG9A at the TGN. What is the functional significance of the ATG9A–AP-4 interaction at the TGN? To address this question, we examined the effect of depleting one component of the interacting pair on the localization of the other. We observed that KO of ATG9A in HeLa cells had no effect on the localization of AP-4 to the TGN (Fig. 2*D*). In contrast, KO of AP-4 ϵ in HeLa cells caused a striking reduction of the dispersed cytoplasmic population of ATG9A and its concentration at the TGN (Fig. 3*A*). A similar redistribution of ATG9A to the TGN was observed upon KO of AP-4 ϵ in the leukemia-derived HAP1 cell line (Fig. 3*B*) and, even more strikingly, in mouse embryonic fibroblasts (MEFs) from AP-4 ϵ KO mice (Fig. 3*C*). For better appreciation of the generality of this redistribution, we show larger fields of cells in Fig. S1. Airyscan superresolution imaging confirmed the tight concentration of ATG9A in the TGN of AP-4 ϵ KO HeLa cells stained for TGN46 and the close apposition of this compartment to the *cis*-Golgi stained for GM130 in AP-4 ϵ KO MEFs (Fig. S2). Transfection of HA-tagged AP-4 ϵ into AP-4 ϵ KO MEFs decreased the concentration of ATG9A at the TGN and restored its more dispersed distribution (Fig. 4*A* and *B*). KD of the ATG9A-interacting μ 4 subunit of AP-4 also caused accumulation of ATG9A at the TGN (Fig. 4*C*). The distributions of giantin, the transferrin receptor (TfR), the cation-independent mannose 6-phosphate receptor (CI-MPR) and the γ -subunit of AP-1 (Fig. 4*D*), in addition to TGN46 and GM130 (Fig. 3), were unchanged in AP-4 ϵ KO cells, indicating that depletion of AP-4 did not cause a general disruption of the Golgi complex or of sorting at the TGN. We also observed that KO of the gene encoding the γ 1 subunit of AP-1, another complex that localizes to the TGN and/or endosomes, had no discernible effect on the overall distribution of ATG9A (Fig. S3). From these experiments, we concluded that AP-4 is specifically required for ATG9A export from the TGN toward peripheral compartments.

Tepsin and AP-5 Are Not Required for ATG9A Exit from the TGN. To date, tepsin is the only well-validated AP-4 accessory protein (10–12). The fact that tepsin possesses two peptide motifs for binding to the ϵ and β 4 subunits of AP-4 (11, 12) makes it potentially capable of cross-linking multiple AP-4 complexes, thereby contributing to the assembly of AP-4 coats. We found, however, that KO of tepsin in HAP1 cells did not alter the distribution of endogenous ATG9A (Fig. 4*E*), indicating that AP-4 does not require tepsin for ATG9 export from the TGN.

AP-5 is another heterotetrameric complex homologous to AP-4, which functions as an adaptor for the putative scaffolding proteins SPG11 and SPG15 (34–36). Importantly for this study, mutations in the genes encoding the ζ -subunit of AP-5 (*AP5Z1*) (37), SPG11 (38), and SPG15 (39) cause HSP with thin corpus callosum, similarly to mutations in AP-4 subunits. Furthermore, both SPG11 and SPG15 have been implicated in autophagy (40, 41). It was therefore of interest to examine whether loss of AP-5 altered ATG9A localization. We found, however, that KO of the AP-5 ζ -subunit in HAP1 cells had no effect on the distribution of endogenous ATG9A between the TGN and peripheral

structures (Fig. 4*F*). This finding is consistent with the proposal that SPG11 and SPG15 function in lysosome reformation after autophagy and not in autophagy initiation (41).

Increased Levels of ATG9A in AP-4 ϵ KO Cells. Immunoblot analyses further revealed that KO of AP-4 ϵ in HeLa, HAP1, and MEF cells increased the levels of ATG9A (Fig. 5*A* and *B*). Conversely, KO of ATG9A in HeLa cells and MEFs had no effect on AP-4 ϵ levels (Fig. 5*A*). We considered the possibility that, by impairing ATG9A transport from the TGN to endosomes and PAS, AP-4 ϵ KO could decrease the turnover of ATG9A in lysosomes or autophagosomes. However, incubation of WT HeLa cells for 3 or 5 h with the vacuolar H⁺ ATPase inhibitor bafilomycin A1, which inhibits lysosomal/autophagosomal degradation (42, 43), did not alter ATG9A levels (Fig. 5*C*). This was in contrast to another autophagy machinery component that is known to undergo lysosomal/autophagosomal degradation, MAP1LC3B (herein referred to as LC3B) (44), which displayed greatly increased levels after incubation of both WT and AP-4 ϵ in HeLa cells treated with bafilomycin A1 (Fig. 5*C*). Finally, incubation with cycloheximide for different times (i.e., cycloheximide chase) followed by immunoblot analysis revealed that ATG9A was highly stable for up to 20 h in both WT and AP-4 ϵ KO HeLa cells (Fig. 5*D*). This was in contrast to LC3B, which was rapidly degraded under the same conditions (Fig. 5*D*). We concluded that KO of AP-4 ϵ increased the levels of ATG9A at steady state in addition to causing its accumulation at the TGN. This increase was not due to decreased lysosomal degradation but most likely to increased synthesis.

Reduced Conversion of LC3B-I to LC3B-II in AP-4 ϵ KO Cells. Because ATG9A plays critical roles in autophagy, reportedly by delivering membranes or lipids to expanding PAS (24–27), we hypothesized that AP-4-deficient cells would exhibit autophagic defects. The most commonly used autophagy reporter is LC3B, which undergoes conversion from a cytosolic, soluble form (LC3B-I) to a lipidated, membrane-bound form (LC3B-II) as a requisite for autophagosome formation (44). Immunoblot analysis of endogenous LC3B indeed revealed several differences between WT and AP-4 ϵ KO cells. First, AP-4 ϵ KO HeLa cells exhibited a 3.2-fold increase in total levels of LC3B (i.e., LC3B-I plus LC3B-II) under basal conditions (Fig. 5*C* and *D*, 0 time points; Fig. 6*A* and *B*; Fig. 6*D*, 0 time points). Second, the basal ratio of LC3B-II to LC3B-I was lower in AP-4 ϵ KO HeLa cells (Fig. 5*C* and *D*, 0 time points; Fig. 6*A* and *C*; Fig. 6*D*, 0 time points) and MEFs (Fig. 6*E*, 0 time points) relative to WT cells. The levels of total LC3B and the ratio of LC3B-II to LC3B-I in AP-4 ϵ KO vs. WT HeLa cells remained different even after treatment of the cells with bafilomycin A1, which blocks autophagic flux (Fig. 5*C*). Finally, the ratio of LC3B-II to LC3B-I was also lower in AP-4 ϵ KO vs. WT HeLa cells and MEFs at all times after induction of autophagy by amino acid and serum starvation (Fig. 6*D* and *E*). Taken together, these experiments indicated that the inability to mobilize ATG9A from the TGN in AP-4 ϵ KO cells impairs LC3B lipidation and induces a compensatory increase in total LC3B expression. Because of this compensation, the absolute amount of LC3B-II in AP-4 ϵ KO HeLa cells and MEFs is maintained or even increased under starvation conditions (LC3B-II band in immunoblots shown in Fig. 6*D* and *E*). In line with this observation, the levels of the autophagosomal cargo receptor SQSTM1 (also known as p62), which is itself degraded by autophagy (45), were not altered in AP-4 ϵ KO HeLa cells (Fig. 6*A*), suggesting that cells were able to overcome the deficiency in ATG9A distribution and LC3B-I processing by up-regulating ATG9A (Fig. 5) and LC3B (Fig. 6). This phenotype contrasted with that of ATG9A KO cells, in which SQSTM1 levels were greatly elevated (Fig. 6*A*).

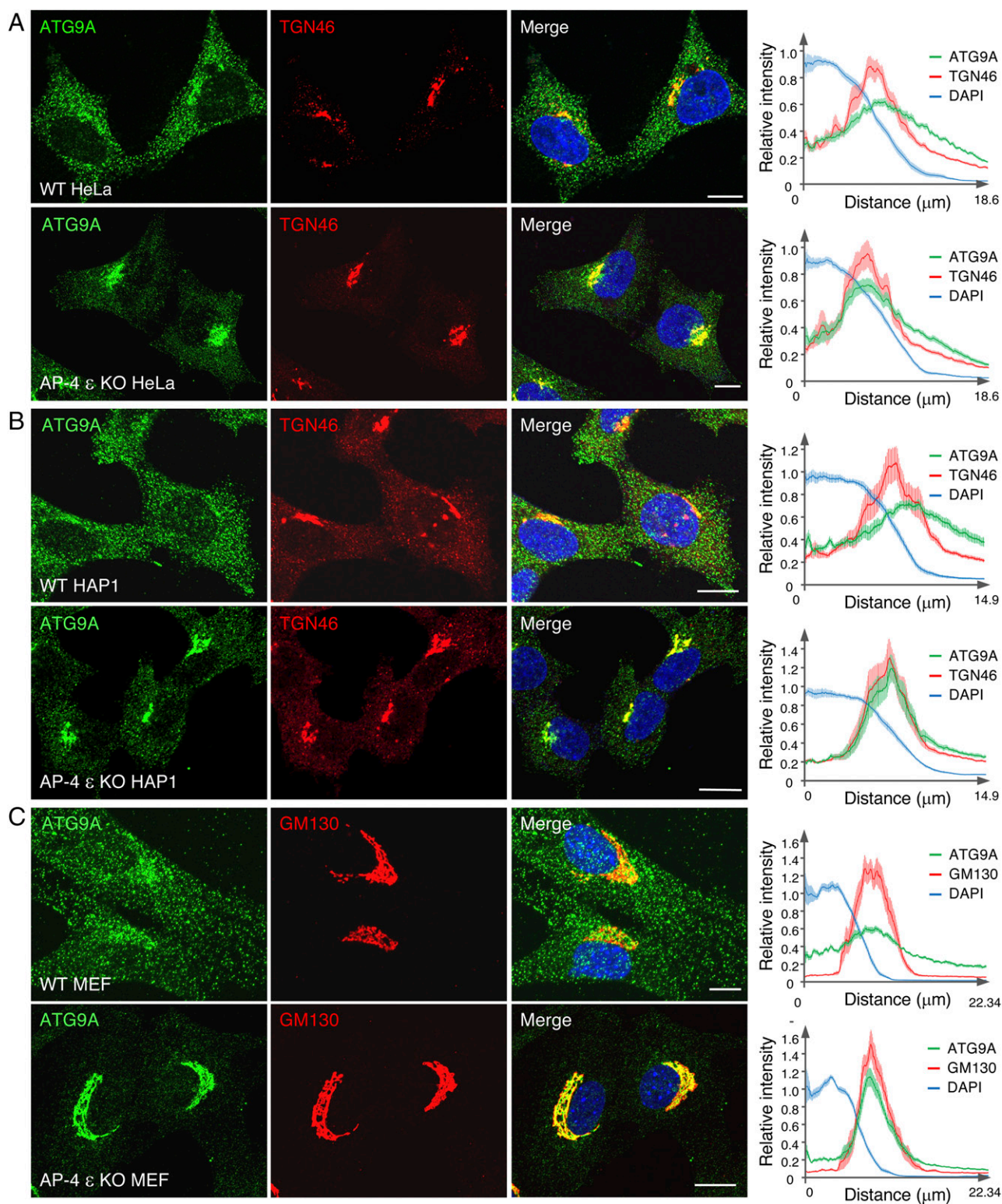


Fig. 3. AP-4 ϵ KO causes accumulation of ATG9A at the TGN. (A–C) Immunofluorescence microscopy of endogenous ATG9A and TGN46 or GM130 in WT or AP-4 ϵ KO HeLa (A), HAP1 (B), or MEF (C) cells. (Scale bars, 10 μm .) The fluorescence intensity for ATG9A (green lines), TGN46 or GM130 (red lines), and DAPI (blue lines) as a function of distance from the center of the cell, measured using the Radial Profile plugin of ImageJ, is shown on the *Right*. Values are the mean \pm SEM of fluorescence intensity relative to the total from 15 cells in each group. Wider fields of cells are shown in Fig. S1. Airyscan microscopy of the colocalization of ATG9A with TGN46 or GM130 is shown in Fig. S2.

Increased Number and Size of LC3B-Positive Structures in AP-4 ϵ KO Cells. Finally, we examined the effect of starvation on the distribution of ATG9A and LC3B in AP-4 ϵ KO MEF. Amino acid

starvation has been shown to cause redistribution of ATG9A from the TGN to peripheral endosomes (25). We observed that the accumulation of ATG9A at the TGN in AP-4 ϵ KO MEFs

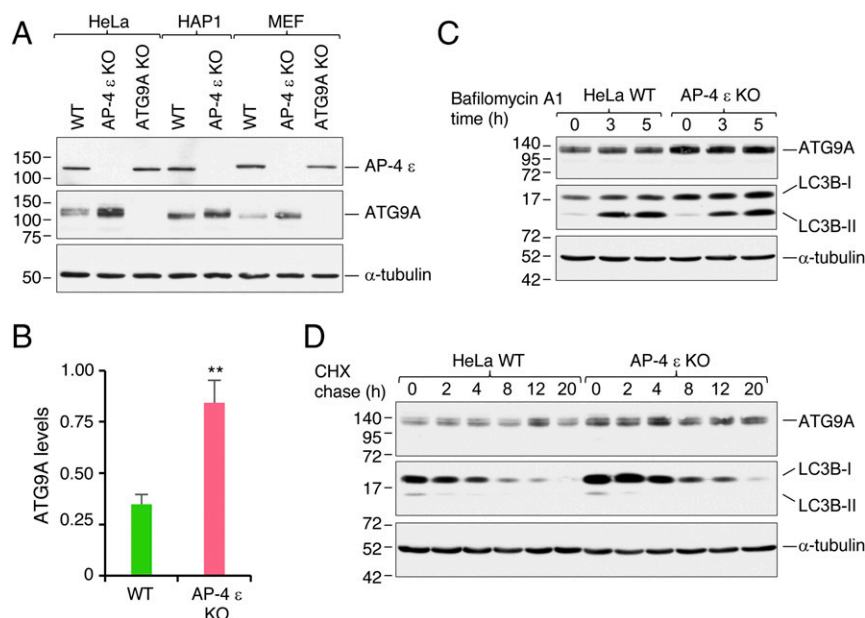


Fig. 5. Increased levels of ATG9A in AP-4 ϵ KO cells. (A) Immunoblot analysis of AP-4 ϵ , ATG9A, and α -tubulin (loading control) in WT, AP-4 ϵ KO, and ATG9A KO HeLa, HAP1 and MEF cells. (B) Quantification of ATG9A relative to α -tubulin levels in HeLa cells from experiments such as that in A. Values are the mean \pm SEM from six independent experiments. $**P < 0.01$. The level of ATG9A in AP-4 KO HeLa cells relative to WT was 2.5 ± 0.2 (mean \pm SEM; $n = 6$). (C) WT and AP-4 ϵ KO HeLa cells were incubated for different times at 37 °C with 100 nM bafilomycin A1 and analyzed by SDS/PAGE and immunoblotting for ATG9A, LC3B, and α -tubulin. (D) WT and AP-4 ϵ KO HeLa cells were incubated for different times at 37 °C with 0.35 mM cycloheximide (CHX) and analyzed by SDS/PAGE and immunoblotting for ATG9A, LC3B, and α -tubulin. In A, C, and D, the positions of molecular mass markers (in kilodaltons) are indicated *Left* of the immunoblots.

was unaltered by amino acid and serum starvation (Fig. 7A). These findings indicated that peripheral redistribution of ATG9A upon starvation requires AP-4.

WT and AP-4 ϵ KO MEFs exhibited faint punctate staining for LC3B in the cytoplasm under basal conditions (Fig. 7B). Amino acid and serum starvation increased LC3B staining in both WT

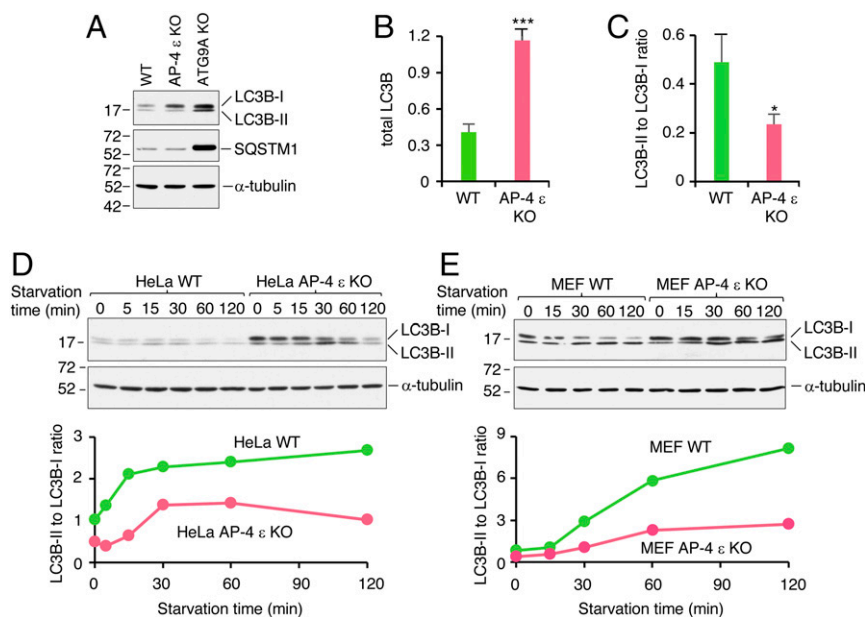


Fig. 6. Increased levels of LC3B and decreased ratio of LC3B-II to LC3B-I in AP-4 ϵ KO cells. (A) Immunoblot analysis of LC3B, SQSTM1, and α -tubulin in WT, AP-4 ϵ KO, and ATG9A KO HeLa cells. (B and C) Quantification of total LC3B (relative to the α -tubulin control) (B) and LC3B-II/LC3B-I ratio under basal conditions in WT and AP-4 ϵ KO HeLa cells (C). Values are the mean \pm SEM from seven assays carried out with samples from six independent experiments (total LC3B) or six assays carried out with samples from five independent experiments (LC3B-II/LC3B-I ratios). $***P < 10^{-4}$; $*P < 0.05$. The total level of LC3B in AP-4 ϵ KO relative to WT HeLa cells was 3.2 ± 0.4 (mean \pm SEM; $n = 7$). (D and E) Effect of amino acid and serum starvation on the conversion of endogenous LC3-I to LC3-II in WT and AP-4 ϵ KO HeLa cells (D) and MEFs (E). Cells were incubated in amino acid- and serum-free DMEM for the indicated times at 37 °C and analyzed by SDS/PAGE and immunoblotting for LC3 and α -tubulin (loading control). The ratio of LC3B-II to LC3B-I was calculated and plotted as a function of time. In A, D, and E, the positions of molecular mass markers (in kilodaltons) are indicated *Left* of the immunoblots.

and AP-4 ϵ KO MEFs (Fig. 7B). However, the number and size of LC3B structures were slightly increased, and LC3B structures were also more irregularly shaped, in AP-4 ϵ KO relative to WT MEFs under both control and starvation conditions (Fig. 7 B and C).

These experiments thus demonstrated that the absence of AP-4 and the resulting concentration of ATG9A at the TGN did not prevent attachment of LC3B to PAS following starvation. However, the number and properties of the LC3B-positive structures were altered, suggesting abnormal PAS maturation.

Discussion

ATG9A is unique among the components of the core autophagy machinery not only for being the only multispinning membrane protein in this group, but also for its property of cycling between a central TGN compartment and various peripheral compartments, including early, recycling, and late endosomes (25–27, 46) as well as PAS (24, 47). The mechanisms that control this cycling, however, are incompletely understood. Particularly lacking is information on how this protein exits the TGN in mammalian cells. In the yeast *Saccharomyces cerevisiae*, export of Atg9 into Golgi-derived vesicles requires the peripheral membrane protein Atg23 and integral membrane protein Atg27 (48, 49). However, these proteins have no known orthologs in mammals. Our findings show instead that exit of ATG9A from the TGN in mammalian cells requires the nonclathrin adaptor complex AP-4.

The requirement of AP-4 for export of ATG9A from the TGN owes to a direct interaction of a YXX \emptyset E motif in the N-terminal tail of ATG9A (i.e., the sequence YQRLE) with the μ 4 subunit of AP-4. This mode of interaction is similar to that of members of the amyloid precursor protein (APP) family, including APP, APLP1, and APLP2, and may likewise involve binding of the YQRLE sequence to a site on β -strands 4, 5, and 6 of the μ 4 C-terminal domain (13). ATG9A also has two loops and a

C-terminal tail facing the cytosol that could harbor additional sorting information (Fig. 1B). Nevertheless, the YXX \emptyset E motif in the N-terminal tail of ATG9A is essential for interaction with the whole AP-4 complex, as demonstrated by the loss of coprecipitation of these proteins upon mutation of the critical Y8 residue in the motif. BLASTP analysis showed that the YXX \emptyset E motif is conserved in ATG9A orthologs from all vertebrate species, in most cases as the exact YQRLE sequence, and in a few cases as YQRLD, in which an aspartate conservatively substitutes the glutamate residue. Vertebrates have a paralogous ATG9B protein with a more restricted pattern of tissue expression (e.g., placenta and pituitary gland in mammals) (50). The sequence of the N-terminal tail of ATG9B is quite divergent from that of ATG9A, but nevertheless it contains a sequence fitting the YXX \emptyset E motif: YERLE in all mammals, and variants such as YRRLE, YHRLE, YQRLE, and YQRID in other vertebrates. These observations suggest evolutionary pressure to conserve this motif in ATG9 isoforms from all vertebrates, presumably because of the need for recognition by the μ 4 subunit of AP-4. In contrast, the *S. cerevisiae* ATG9A ortholog does not have a YXX \emptyset E motif and this species also lacks an AP-4 complex, consistent with the interdependence of both elements of this signal–adaptor interaction. We speculate that yeast ancestors may have lost this sorting mechanism because the small size of the cells does not necessitate deployment of Atg9 far away from the Golgi complex.

The YQRLE sequence in ATG9A has also been shown to interact with the related AP-1 and AP-2 complexes (27, 30), although, in our experiments, interactions with the corresponding μ 1 and μ 2 subunits were weaker than those with μ 4, as evidenced by their inability to support yeast growth in Y2H assays performed under high stringency conditions (i.e., high concentrations of 3-amino-1,2,4-triazole) (AT) (Fig. 1C). The interaction with AP-2 likely mediates internalization of ATG9A from the cell surface for delivery to endosomes and PAS (27, 32, 33). The significance of the

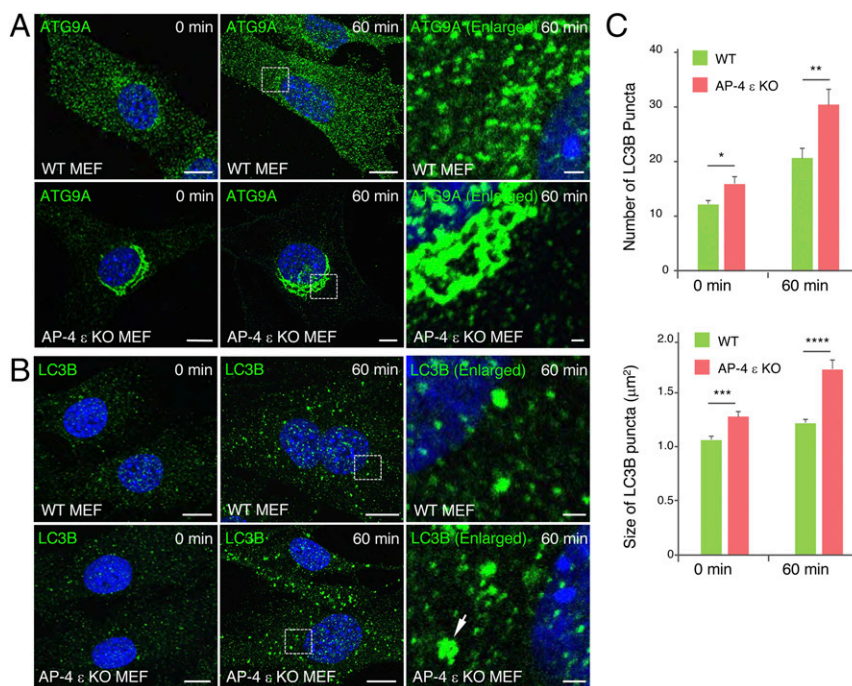


Fig. 7. Abnormal LC3B structures in starved AP-4 ϵ KO cells. (A and B) Immunofluorescence microscopy for endogenous ATG9A (A) or LC3B (B) in WT and AP-4 ϵ KO MEFs incubated for 0 or 60 min in amino acid- and serum-free DMEM. Images in the *Right* column are magnifications of the boxed areas. (Scale bars, 10 μm ; enlarged images at *Right*, 1 μm .) The arrow indicates the irregular shape of an LC3B structure. (C) Quantification of the number and size of LC3 puncta from experiments such as that in B using ImageJ with Analyze Particles. Values are the mean \pm SEM from 20 cells per sample. * P < 0.05, ** P < 0.01, *** P < 0.001, **** P < 1×10^{-5} .

interaction with AP-1 (30) is less clear. Guo et al. (31) showed that KD of the AP-1 γ 1 subunit reduced starvation-induced autophagosome formation, but the role of AP-1 in ATG9A trafficking was not addressed. We observed that AP-1 γ 1 KO did not alter the distribution of ATG9A between the TGN and peripheral compartments (Fig. S3), suggesting that AP-1 is not involved in ATG9A exit from the TGN but possibly in a different transport step.

Given that tepsin has the potential to cross-link multiple AP-4 heterotetramers (11), we hypothesized that it could also participate in ATG9A trafficking. However, we found that tepsin is not required for export of ATG9A from the TGN. This finding, plus the fact that AP-4 does not depend on tepsin for association with the TGN (10), is most consistent with tepsin being a truly accessory protein. As is the case for other ENTH and VHS domain-containing proteins that function in association with clathrin coats (51, 52), the function of tepsin may be to expand the repertoire of cargos that are sorted by AP-4 coats.

The accumulation of ATG9A at the TGN in AP-4 KO or KD cells has functional consequences. A striking phenotype is the decreased ratio of lipidated LC3B-II to cytosolic LC3B-I under both basal and starvation conditions. ATG9A is thought to function to deliver membranes and/or lipids to the growing phagophores (26, 48). Our results indicate that this process partially contributes to LC3B lipidation. However, cells appear to compensate for this deficiency by increasing the levels of both ATG9A and total LC3B. As a result, the absolute amounts of LC3B-II are not diminished but moderately elevated in HeLa cells and MEFs under starvation conditions. Consistent with this, staining for LC3B is somewhat stronger in AP-4 ϵ KO MEFs relative to WT MEFs under starvation conditions. These compensatory events may account for the observation that AP-4 ϵ KO HeLa cells, in contrast to ATG9A KO cells, have normal levels of SQSTM1. Despite this compensation, AP-4 ϵ KO MEFs exhibit an abnormal number and morphology of LC3B-positive structures. The up-regulation of ATG9A and LC3B may thus mitigate some but not all autophagy defects in AP-4 ϵ KO cells, particularly under starvation conditions.

ATG9A KO cells have more severe autophagic defects than those of the AP-4 ϵ KO cells described here (53, 54). This difference may explain why ATG9A KO mice die embryonically or postnatally (53, 55, 56), whereas AP-4 β 4 KO mice are viable (17). This may also be the reason why AP-4-deficient patients survive to adulthood, albeit with serious neurological problems. These problems could arise from missorting of AP-4 cargos such as AMPAR (17) or APP family members (13), which play important roles in neurodevelopment and synaptic function (57, 58). However, it is likely that the missorting of ATG9A and consequent autophagic defects reported here might also contribute to the

pathogenesis of this type of complicated HSP. In light of our findings, the accumulation of AMPAR in autophagosomes of AP-4 β 4 KO mice could result not just from missorting of AMPAR to the axon but also from impaired degradation of AMPAR in autophagosomes. It is worth noting that other HSPs, such as SPG11, SPG15, and SPG49, are also associated with autophagic defects (40, 41, 59, 60). SPG49, in particular, is caused by mutation in an LC3B-interacting protein, TECPR2, and cells from SPG49 patients show decreased LC3B-II levels (59). Moreover, altered autophagy is thought to contribute to neurodegenerative disorders such as Alzheimer's, Parkinson's, and Huntington's diseases, amyotrophic lateral sclerosis, and spinal muscular atrophy, among others (61). A likely explanation is that impaired autophagy prevents the clearance of protein aggregates or damaged organelles, which are particularly toxic to neurons. We think that the special vulnerability of neurons to autophagy dysfunction could account for the neurological manifestations of AP-4 deficiency.

In sum, our studies have identified ATG9A as a specific cargo for AP-4. The export of ATG9A from the TGN to peripheral compartments mediated by AP-4 promotes the early stages of autophagosome formation. Some of these peripheral compartments are part of the endosomal system (25–27, 46) and, consequently, AP-4-mediated export represents a form of anterograde transport. Other peripheral compartments containing ATG9A, however, correspond to PAS that arise in association with the endoplasmic reticulum (ER) (62), ER–Golgi intermediate compartment (ERGIC) (63), or mitochondria (64). Could AP-4 then be considered to mediate some kind of retrograde transport, as is the case for the related COPI coat (65)? Answers to this and other questions concerning the transport of ATG9A will require a better understanding of the connections between all of the compartments through which ATG9A traffics in the performance of its function.

Materials and Methods

Recombinant DNA constructs, antibodies, cell lines, yeast two-hybrid assays, cell transfection, RNA interference, immunoprecipitation and immunoblotting, amino acid and serum starvation, bafilomycin and cycloheximide treatment, immunofluorescence microscopy, and image and statistical analysis are described in *SI Materials and Methods*. All animal procedures were conducted under protocol 15-021 approved by the National Institute of Child Health and Human Development Animal Care and Use Committee.

ACKNOWLEDGMENTS. We thank Rui Jia for helpful discussions; Christina Schindler, Dennis Drayna, and Shizuo Akira for kind gifts of reagents; and Yuna Lee for help with the Y2H assays. This work was supported by the intramural program of the National Institute of Child Health and Human Development, NIH (project ZIA HD001607).

- Bonifacino JS, Glick BS (2004) The mechanisms of vesicle budding and fusion. *Cell* 116:153–166.
- Park SY, Guo X (2014) Adaptor protein complexes and intracellular transport. *Biosci Rep* 34:e00123.
- Dacks JB, Robinson MS (2017) Outerwear through the ages: Evolutionary cell biology of vesicle coats. *Curr Opin Cell Biol* 47:108–116.
- Dell'Angelica EC, Mullins C, Bonifacino JS (1999) AP-4, a novel protein complex related to clathrin adaptors. *J Biol Chem* 274:7278–7285.
- Hirst J, Bright NA, Rous B, Robinson MS (1999) Characterization of a fourth adaptor-related protein complex. *Mol Biol Cell* 10:2787–2802.
- Shih W, Gallusser A, Kirchhausen T (1995) A clathrin-binding site in the hinge of the beta 2 chain of mammalian AP-2 complexes. *J Biol Chem* 270:31083–31090.
- Traub LM, Kornfeld S, Ungewickell E (1995) Different domains of the AP-1 adaptor complex are required for Golgi membrane binding and clathrin recruitment. *J Biol Chem* 270:4933–4942.
- Dell'Angelica EC, et al. (1997) AP-3: An adaptor-like protein complex with ubiquitous expression. *EMBO J* 16:917–928.
- Boehm M, Aguilar RC, Bonifacino JS (2001) Functional and physical interactions of the adaptor protein complex AP-4 with ADP-ribosylation factors (ARFs). *EMBO J* 20:6265–6276.
- Borner GH, et al. (2012) Multivariate proteomic profiling identifies novel accessory proteins of coated vesicles. *J Cell Biol* 197:141–160.
- Mattera R, Guardia CM, Sidhu SS, Bonifacino JS (2015) Bivalent motif-ear interactions mediate the association of the accessory protein tepsin with the AP-4 adaptor complex. *J Biol Chem* 290:30736–30749.
- Frazier MN, et al. (2016) Molecular basis for the interaction between AP4 β 4 and its accessory protein, tepsin. *Traffic* 17:400–415.
- Burgos PV, et al. (2010) Sorting of the Alzheimer's disease amyloid precursor protein mediated by the AP-4 complex. *Dev Cell* 18:425–436.
- Choy RW, Cheng Z, Schekman R (2012) Amyloid precursor protein (APP) traffics from the cell surface via endosomes for amyloid β (A β) production in the trans-Golgi network. *Proc Natl Acad Sci USA* 109:E2077–E2082.
- Ross BH, Lin Y, Corales EA, Burgos PV, Mardones GA (2014) Structural and functional characterization of cargo-binding sites on the μ 4-subunit of adaptor protein complex 4. *PLoS One* 9:e88147.
- Toh WH, Tan JZ, Zulkefli KL, Houghton FJ, Gleeson PA (2017) Amyloid precursor protein traffics from the Golgi directly to early endosomes in an Arl5b- and AP4-dependent pathway. *Traffic* 18:159–175.
- Matsuda S, et al. (2008) Accumulation of AMPA receptors in autophagosomes in neuronal axons lacking adaptor protein AP-4. *Neuron* 57:730–745.
- Yap CC, et al. (2003) Adaptor protein complex-4 (AP-4) is expressed in the central nervous system neurons and interacts with glutamate receptor delta2. *Mol Cell Neurosci* 24:283–295.
- Moreno-De-Luca A, et al. (2011) Adaptor protein complex-4 (AP-4) deficiency causes a novel autosomal recessive cerebral palsy syndrome with microcephaly and intellectual disability. *J Med Genet* 48:141–144.
- Verkerk AJ, et al. (2009) Mutation in the AP4M1 gene provides a model for neuroaxonal injury in cerebral palsy. *Am J Hum Genet* 85:40–52.

21. Abou Jamra R, et al. (2011) Adaptor protein complex 4 deficiency causes severe autosomal-recessive intellectual disability, progressive spastic paraplegia, shy character, and short stature. *Am J Hum Genet* 88:788–795.
22. Blackstone C (2012) Cellular pathways of hereditary spastic paraplegia. *Annu Rev Neurosci* 35:25–47.
23. Rubinsztein DC, Shpilka T, Elazar Z (2012) Mechanisms of autophagosome biogenesis. *Curr Biol* 22:R29–R34.
24. Reggiori F, Tucker KA, Stromhaug PE, Klionsky DJ (2004) The Atg1-Atg13 complex regulates Atg9 and Atg23 retrieval transport from the pre-autophagosomal structure. *Dev Cell* 6:79–90.
25. Young AR, et al. (2006) Starvation and ULK1-dependent cycling of mammalian Atg9 between the TGN and endosomes. *J Cell Sci* 119:3888–3900.
26. Orsi A, et al. (2012) Dynamic and transient interactions of Atg9 with autophagosomes, but not membrane integration, are required for autophagy. *Mol Biol Cell* 23:1860–1873.
27. Imai K, et al. (2016) Atg9A trafficking through the recycling endosomes is required for autophagosome formation. *J Cell Sci* 129:3781–3791.
28. Mellacheruvu D, et al. (2013) The CRAPome: A contaminant repository for affinity purification-mass spectrometry data. *Nat Methods* 10:730–736.
29. Traub LM, Bonifacino JS (2013) Cargo recognition in clathrin-mediated endocytosis. *Cold Spring Harb Perspect Biol* 5:a016790.
30. Zhou C, et al. (2017) Regulation of mATG9 trafficking by Src- and ULK1-mediated phosphorylation in basal and starvation-induced autophagy. *Cell Res* 27:184–201.
31. Guo Y, et al. (2012) AP1 is essential for generation of autophagosomes from the trans-Golgi network. *J Cell Sci* 125:1706–1715.
32. Puri C, Renna M, Bento CF, Moreau K, Rubinsztein DC (2013) Diverse autophagosome membrane sources coalesce in recycling endosomes. *Cell* 154:1285–1299.
33. Popovic D, Dikic I (2014) TBC1D5 and the AP2 complex regulate ATG9 trafficking and initiation of autophagy. *EMBO Rep* 15:392–401.
34. Slabicki M, et al. (2010) A genome-scale DNA repair RNAi screen identifies SPG48 as a novel gene associated with hereditary spastic paraplegia. *PLoS Biol* 8:e1000408.
35. Hirst J, et al. (2011) The fifth adaptor protein complex. *PLoS Biol* 9:e1001170.
36. Hirst J, et al. (2013) Interaction between AP-5 and the hereditary spastic paraplegia proteins SPG11 and SPG15. *Mol Biol Cell* 24:2558–2569.
37. Hirst J, et al. (2015) Loss of AP-5 results in accumulation of aberrant endolysosomes: Defining a new type of lysosomal storage disease. *Hum Mol Genet* 24:4984–4996.
38. Stevanin G, et al. (2007) Mutations in SPG11, encoding spatacsin, are a major cause of spastic paraplegia with thin corpus callosum. *Nat Genet* 39:366–372.
39. Hanein S, et al. (2008) Identification of the SPG15 gene, encoding spastizin, as a frequent cause of complicated autosomal-recessive spastic paraplegia, including Kjellin syndrome. *Am J Hum Genet* 82:992–1002.
40. Vantaggiato C, et al. (2013) Defective autophagy in spastizin mutated patients with hereditary spastic paraparesis type 15. *Brain* 136:3119–3139.
41. Chang J, Lee S, Blackstone C (2014) Spastic paraplegia proteins spastizin and spatacsin mediate autophagic lysosome reformation. *J Clin Invest* 124:5249–5262.
42. Swallow CJ, Grinstein S, Rotstein OD (1990) A vacuolar type H(+)-ATPase regulates cytoplasmic pH in murine macrophages. *J Biol Chem* 265:7645–7654.
43. Takeshige K, Baba M, Tsuboi S, Noda T, Ohsumi Y (1992) Autophagy in yeast demonstrated with proteinase-deficient mutants and conditions for its induction. *J Cell Biol* 119:301–311.
44. Kabeya Y, et al. (2004) LC3, GABARAP and GATE16 localize to autophagosomal membrane depending on form-II formation. *J Cell Sci* 117:2805–2812.
45. Bjørkøy G, et al. (2005) p62/SQSTM1 forms protein aggregates degraded by autophagy and has a protective effect on huntingtin-induced cell death. *J Cell Biol* 171:603–614.
46. Puri C, Renna M, Bento CF, Moreau K, Rubinsztein DC (2014) ATG16L1 meets ATG9 in recycling endosomes: Additional roles for the plasma membrane and endocytosis in autophagosome biogenesis. *Autophagy* 10:182–184.
47. Reggiori F, Shintani T, Nair U, Klionsky DJ (2005) Atg9 cycles between mitochondria and the pre-autophagosomal structure in yeasts. *Autophagy* 1:101–109.
48. Yamamoto H, et al. (2012) Atg9 vesicles are an important membrane source during early steps of autophagosome formation. *J Cell Biol* 198:219–233.
49. Backues SK, et al. (2015) Atg23 and Atg27 act at the early stages of Atg9 trafficking in *S. cerevisiae*. *Traffic* 16:172–190.
50. Yamada T, et al. (2005) Endothelial nitric-oxide synthase antisense (NOS3AS) gene encodes an autophagy-related protein (APG9-like2) highly expressed in trophoblast. *J Biol Chem* 280:18283–18290.
51. Legendre-Guillemin V, Wasiaik S, Hussain NK, Angers A, McPherson PS (2004) ENTH/ANTH proteins and clathrin-mediated membrane budding. *J Cell Sci* 117:9–18.
52. Bonifacino JS (2004) The GGA proteins: Adaptors on the move. *Nat Rev Mol Cell Biol* 5:23–32.
53. Saitoh T, et al. (2009) Atg9a controls dsDNA-driven dynamic translocation of STING and the innate immune response. *Proc Natl Acad Sci USA* 106:20842–20846.
54. Kishi-Itakura C, Koyama-Honda I, Itakura E, Mizushima N (2014) Ultrastructural analysis of autophagosome organization using mammalian autophagy-deficient cells. *J Cell Sci* 127:4089–4102.
55. Kojima T, et al. (2015) Role of the Atg9a gene in intrauterine growth and survival of fetal mice. *Reprod Biol* 15:131–138.
56. Yamaguchi J, et al. (May 17, 2017) Atg9a deficiency causes axon-specific lesions including neuronal circuit dysgenesis. *Autophagy*, 10.1080/15548627.2017.1314897.
57. Malinow R, Malenka RC (2002) AMPA receptor trafficking and synaptic plasticity. *Annu Rev Neurosci* 25:103–126.
58. Müller UC, Zheng H (2012) Physiological functions of APP family proteins. *Cold Spring Harb Perspect Med* 2:a006288.
59. Oz-Levi D, et al. (2012) Mutation in TECPR2 reveals a role for autophagy in hereditary spastic paraparesis. *Am J Hum Genet* 91:1065–1072.
60. Varga RE, et al. (2015) In vivo evidence for lysosome depletion and impaired autophagic clearance in hereditary spastic paraplegia type SPG11. *PLoS Genet* 11:e1005454.
61. Nixon RA (2013) The role of autophagy in neurodegenerative disease. *Nat Med* 19:983–997.
62. Dunn WA, Jr (1990) Studies on the mechanisms of autophagy: Formation of the autophagic vacuole. *J Cell Biol* 110:1923–1933.
63. Ge L, Zhang M, Schekman R (2014) Phosphatidylinositol 3-kinase and COPII generate LC3 lipidation vesicles from the ER-Golgi intermediate compartment. *Elife* 3:e04135.
64. Hailey DW, et al. (2010) Mitochondria supply membranes for autophagosome biogenesis during starvation. *Cell* 141:656–667.
65. Cosson P, Letourneur F (1994) Coatamer interaction with di-lysine endoplasmic reticulum retention motifs. *Science* 263:1629–1631.
66. Guo X, et al. (2013) The adaptor protein-1 μ B subunit expands the repertoire of basolateral sorting signal recognition in epithelial cells. *Dev Cell* 27:356–366.
67. Cong L, et al. (2013) Multiplex genome engineering using CRISPR/Cas systems. *Science* 339:819–823.
68. Chen Y, Gershlick DC, Park SY, Bonifacino JS (October 4, 2017) Segregation in the Golgi complex precedes export of endolysosomal proteins in distinct transport carriers. *J Cell Biol*, 10.1083/jcb.201707172.
69. Mattera R, Arighi CN, Lodge R, Zerial M, Bonifacino JS (2003) Divalent interaction of the GGAs with the Rabaptin-5-Rabex-5 complex. *EMBO J* 22:78–88.
70. Mattera R, Bonifacino JS (2008) Ubiquitin binding and conjugation regulate the recruitment of Rabex-5 to early endosomes. *EMBO J* 27:2484–2494.